Aspects of Electrokinetic Charging in Liquid Microjets

Wendy L. Holstein, Laurel J. Hayes, Ella M. C. Robinson, Gerald S. Laurence, and Mark A. Buntine*

Department of Chemistry, The University of Adelaide, South Australia 5005, Australia

Received: November 6, 1998; In Final Form: February 3, 1999

We have investigated the physicochemical basis of electrokinetic charge separation in methanol using micron-sized channel diameters under both turbulent and laminar flow conditions. Turbulent flow studies were conducted using a 40 μm diameter stainless steel aperture which had a channel length of 0.5 mm. Under these conditions, electrokinetic streaming currents arose from a charge stripping process in the region close to the aperture channel wall. The moving liquid removed the relatively weakly held charges from the outer portion of the electrical double layer formed at the solid−liquid interface. Streaming currents were simultaneously measured at both the conducting aperture and a downstream copper plate. The magnitudes of the streaming currents were shown to be equal at the aperture and the plate; however, the sign of the current at each measurement location was opposite. The magnitude of the streaming currents varied quadratically with mean liquid flow velocity. Studies under laminar flow conditions were conducted using a 3 cm length of fused silica capillary which had an internal diameter of 25 μm. Under laminar flow conditions at higher flow velocities through the nonconducting fused silica channel, the extent of charge separation was ultimately limited by the extent to which excess charge built up within the capillary could be neutralized. We develop a simple model that shows how an interplay between fluid flow, ion mobility, and solid−liquid interfacial chemistry influences the extent of electrokinetic charging in the fused silica channels.

1. Introduction

A topic of considerable continuing interest**,** concerns the microscopic structure and dynamics of solute molecules (neutrals or ions) in the presence of a solvent. Generally, three distinct experimental approaches have been employed to directly probe microscopic solute−solvent behavior. Optical interrogation of bulk condensed-phase samples through, for example, ultrafast spectroscopies[1−4] and interfacial harmonic generation techniques[5−10] has yielded a wealth of detailed information on the microscopic environments experienced by solute and solvent alike. Experiments involving the scattering of electrons[11,12] and particles[13,14] from thin liquid films prepared under high-vacuum conditions have also greatly advanced our understanding of the electronic and molecular structure of condensed-phase species. Still other experimental approaches have focused on introducing the condensed-phase sample into the gas phase where an extensive armory of techniques for microscopic structural interrogation is available to the researcher.

Most approaches designed to introduce normally condensed-phase species into the gas phase have made use of a molecular beam in some way. For example, supersonic expansions into high vacuum allow for the extremely efficient cooling of mixtures of gaseous samples down to temperatures of only a few tens of kelvin.[15] At these ultralow temperatures, clustering of the gaseous molecules forms microsolvated moieties where individual solute−solvent interactions can be explored.[16−25] The use of supersonic free jet expansions continues to be a fruitful experimental approach designed to bridge the gap between gaseous and condensed-phase environments. However, a more novel approach to introducing condensed-phase samples into the gas phase relies upon injecting a very thin, fast-moving liquid jet into a high vacuum. The resultant liquid microjet is often called a "liquid beam" and its experimental use is becoming increasingly popular. It is prudent, therefore, to spend a little effort in learning more about the basic physicochemical processes at play as a liquid microjet is formed.

One of the earliest reports describing the generation of a liquid beam under high vacuum conditions was given by Siegbahn,[26] who has continued to utilize the technique for over 20 years to study the X-ray photoelectron spectroscopy of liquid surfaces. Other practitioners of the technique include Keller et al.,[27−29] Yamamoto and Nishi,[30−32] Faubel and co-workers,[33−37] and Kondow.[38−50]

A powerful motivation for the development of the liquid beam methodology has been to provide a means of probing evaporation from a fresh, clean, continuously renewed liquid surface without interference from the equilibrium vapor immediately above the surface.[26,33,34] Several interesting surface chemistry observations have been made in this regard. For example, from the velocity distributions of water molecules evaporating from the clean liquid surface, Faubel and co-workers found that the surface of a water liquid beam is supercooled to temperatures less than 210 K.[33] In a very recent report describing photoelectron studies of a liquid microjet of pure water, Faubel et al. point to the observation of a molecular alignment of the dipole moment of surface H_2O. They propose that the water molecules at the liquid surface are preferentially oriented such that the H atoms point away from the bulk.[37]

Analysis of the photoelectron spectra collected from liquid microjets has shown them to be influenced by the presence of a surface charge which is generated by a charge separation process within the streaming liquid as it passes through a microjet nozzle aperture.[37] Faubel et al. report that the electro-

* Address correspondence to this author. Fax: +61 8 8303 4358. E-mail: mbuntine@chemistry.adelaide.edu.au.

10.1021/jp984336v CCC: $18.00
Published on Web 03/27/1999

kinetic streaming potential, which can accelerate or retard photoelectrons from the liquid surface, is given by

$$\Phi_{str} = -\frac{1}{2\pi\epsilon_0}\frac{I_{str}}{v_{jet}}\ln\left(\frac{d_{jet}}{2}\right) \quad (1)$$

Here, I_{str} is the measured electrokinetic streaming current, v_{jet} is the liquid streaming velocity, and d_{jet} is the diameter of the nozzle aperture. The electrokinetic streaming potential is found to shift only the zero reference potential of the photoelectron spectra, so long as operation of the liquid microjet remains stable.[37]

The charge separation process which brings about the manifestation of an electrokinetic streaming current is well-known[51,52] and occurs within the nozzle aperture. The interaction between the hydrodynamic fluid velocity profile and the electrical double layer generated at the liquid−nozzle interface is given by[35,37,52,53]

$$I_{str} = \int_0^r \rho(r)\cdot u(r)\, dr \quad (2)$$

where $\rho(r)$ is the ion charge density, $u(r)$ is the hydrodynamic velocity profile, and r is the radius of the nozzle channel. The form of the above expression is strictly true only for laminar flow conditions. However, even if the fluid flow is so fast as to be turbulent elsewhere, the expression will hold if the fluid flow is laminar in the thin sublayer near the nozzle wall.[52]

Inspection of eq 2 shows that the extent of charge separation can be influenced by varying both the hydrodynamic velocity profile and the electrical boundary layer thicknesses. Consistent with this model, Faubel et al.[36,37] control the hydrodynamic layer by varying the fluid flow velocity through the nozzle aperture. They also control the electrical double layer by adjusting the pH of the liquid and the temperature of the liquid (which affects the self-dissociation of the liquid). An interesting result from these workers[35] is that the streaming currents vary widely in both sign and magnitude as a function of the liquid beam velocity and solution pH. Variations in the sign of the electrokinetic streaming current as a function of pH are attributed to the differing ionic mobilities of H^+ and OH^- ions in solution.[35−37]

In this paper we report on a series of experiments designed to more fully understand the electrokinetic charging of liquid beams. We show how the magnitude of electrokinetic charging depends not only on the bulk flow velocity of the liquid beam, but also on the type of fluid flow (turbulent or laminar) and solute ion concentration. In the particular case of laminar flow we present a simple model to show how the surface chemistry within the nozzle capillary has a profound influence on the magnitude of the electrokinetic streaming currents generated.

2. Experimental Section

A schematic illustration of the liquid microjet apparatus is presented in Figure 1. Two configurations of the liquid microjet nozzle have been developed. In the first configuration the liquid emerges from a 0.5 mm thick stainless steel aperture (Lennox Laser) into a vacuum chamber equipped with an Edwards Diffstak Model 160/700, 700 L/s diffusion pump. Nozzle diameters range in size from 5 to 40 μm, although most data were collected with 40 μm apertures. A constant flow of liquid through the nozzle aperture is supplied by a Waters Model 590 programmable solvent delivery pump. The pump is fitted with flow dampening modules to minimize oscillations in the flow rate as we have observed that the electrokinetic streaming currents are extremely sensitive to variations in flow rate. A

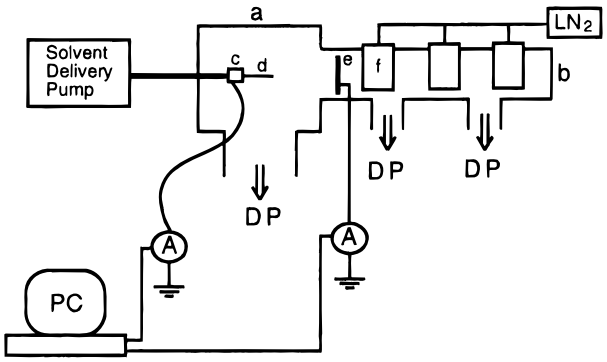

Figure 1. Schematic illustration of the liquid microjet apparatus. Legend: (a) source chamber, (b) condensation chamber, (c) liquid beam nozzle, (d) liquid beam, (e) downstream copper plate, (f) liquid nitrogen filled condensation traps. Electrokinetic streaming currents are recorded by picoammeters connected to the nozzle aperture and/or the downstream copper plate. The experiment is controlled and data is collected by a personal computer.

0.2 micron porous filter designed to prevent clogging of the nozzle aperture is placed in series with the flow dampening modules. Liquid flow rates of between 0.4 and 1.0 mL/min are used. Under these conditions turbulent flow through the aperture results. In order to undertake the streaming current measurements at the nozzle aperture, a 2 cm long Teflon or PEEK block is used to electrically isolate the nozzle.

In the second nozzle configuration, the thin stainless steel aperture is replaced by a 3 cm length of 25 μm internal diameter fused silica capillary tubing (SGE). The significantly longer channel allows for laminar flow conditions to be established. Fused silica tubing is used in these experiments as it is readily available as a gas chromotography consumable and is relatively inexpensive. We have observed quite different behavior in the streaming currents under turbulent and laminar flow conditions. Liquid flow rates of between 0.2 and 1.2 mL/min are used in the laminar flow studies.

When the liquid jet is in operation, the pressure in the source chamber is typically $10^{-4}-10^{-5}$ Torr, depending upon the size of the nozzle aperture and the liquid flow rate. Lower source chamber pressures are maintained by cooling a 5 cm diameter copper plate (placed above the throat of the diffusion pump) with liquid nitrogen. In order to prevent the liquid beam from freezing at very low flow rates, the liquid is flowed through the nozzle while the chamber is evacuated.

Approximately 8 cm downstream from the nozzle the liquid beam passes through a 1.5 cm orifice into the condensation chamber. Here, up to three 6 × 19 cm cylindrical stainless steel traps filled with liquid nitrogen act as a cryropumping/condensation unit for the liquid beam. The condensation chamber is pumped by two Edwards Model E02, 150 L/s diffusion pumps in order to maintain an ambient pressure approximately equal to that in the source chamber. Typically, the liquid beam can be operated for approximately 2.25 h before the condensation traps need to be removed and cleaned.

For the turbulent flow aperture, electrokinetic streaming currents are recorded at both the stainless steel nozzle and an electrically isolated copper plate located 20 cm downstream from the nozzle. The fused silica capillary used to generate laminar flow conditions allows for streaming currents to be observed only at the copper plate. Streaming currents are measured with a pair of Keithly Model 410A picoammeters. Output from the picoammeters is passed through an analog-to-digital converter (National Instruments, LabPC+) and recorded on a personal computer.

The electrical conductivity of the solutions is measured before their injection into the vacuum chamber. Solution conductivities are measured with a Philips PW9527 digital conductivity meter. Unless otherwise specified, all experiments are conducted using twice-distilled methanol. For studies investigating the effect of H^+ concentration on streaming currents under laminar flow conditions, concentrated hydrochloric acid is added to the twice-distilled methanol.

3. Results and Discussion

3.1. Turbulent Flow. Electrokinetic streaming currents were measured for twice-distilled methanol under turbulent flow conditions using a 0.5 mm thick stainless steel aperture as the liquid microjet nozzle. Characterization of the type of fluid flow in a tube as being either turbulent or laminar is usually made on the basis of calculating the Reynolds number[54] for the flow. The Reynolds number is defined as

$$R_e = 2\upsilon r\rho/\eta \tag{3}$$

where υ is the average velocity of the fluid, r is the radius of the tube, ρ is the fluid density, and η is the fluid viscosity. It is a generally accepted guide that if the (dimensionless) Reynolds number is below about 2000, the flow is laminar, while any value exceeding 2000 indicates turbulent flow.[54] Under our experimental conditions, the slowest (and therefore least likely to be turbulent) flow was achieved using a 40 μm diameter aperture and a fluid flow rate of 0.4 mL/min. Methanol has a density of 787 kg m^{-3} at a temperature of 298 K,[55] and a viscosity of 5.47×10^{-4} kg m^{-1} s^{-1}.[56] Therefore, the flow has a corresponding Reynolds number of 305 and we might expect laminar flow to be occurring. However, the above analysis does not consider the fact that laminar flow is not fully developed because the length of the aperture is so small. The characteristic distance required for the development of laminar flow in short lengths of tubing is given by the phenomenonological relationship[57]

$$h \approx 0.1rR_e \tag{4}$$

where h is the characteristic input length required to establish laminar flow, r is the radius of the tube, and R_e is the Reynolds number defined in eq 3. With an aperture radius of 20 μm and a Reynolds number of 305, the characteristic length required to establish laminar flow is 0.6 mm. The stainless steel aperture has a total thickness of only 0.5 mm, so we can conclude that the flow of methanol through the thin aperture is indeed turbulent. Such a conclusion is consistent with the work of Abedian and Sonin[58] who conclude that a minimum channel length of approximately 10^3 radii is required to establish laminar flow conditions.

In Figure 2 we present the variation of streaming current with flow velocity under conditions of turbulent flow through a 40 μm diameter aperture. The streaming currents were measured at both the aperture itself and at an electrically isolated copper plate located 20 cm downstream of the nozzle (see Figure 1). The lowest fluid flow rate used for these measurements was 0.4 mL/min, corresponding to a bulk flow velocity of 5.3 m/s. At flow rates less than 0.4 mL/min, the liquid microjet ceased to operate. Instead, small liquid drops formed around the exit of the nozzle with solvent evaporation rapidly freezing the nozzle channel closed. The highest fluid flow rate used was 1.0 mL/min, corresponding to a bulk flow velocity of 13.2 m/s. At flow rates greater than 1.0 mL/min, the liquid microjet broke up into a fine aerosol (due to Rayleigh instabilities in the beam) and dissipated prior to reaching the downstream copper plate.

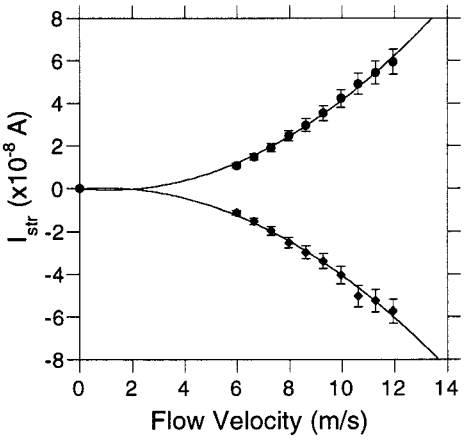

Figure 2. Variation of the electrokinetic streaming current with fluid flow velocity. Data are collected under turbulent flow conditions generated by passing twice-distilled methanol through a 0.5 mm thick, 40 μm diameter stainless steel aperture. Legend: (●) aperture current, (◆) plate current. Error bars represent one standard deviation. The streaming current at the aperture is measured directly with a picoammeter. The streaming current generated by excess charge carried away by the liquid beam is measured by a picoammeter connected to an electrically isolated copper plate located 20 cm downstream from the nozzle.

The first observation to be made from Figure 2 is that the magnitude of the electrokinetic streaming current measured at the downstream plate is equal to that measured at the aperture itself. Indeed, the streaming currents are seen to be equal in magnitude and opposite in sign. Equation 2 indicates that for a given liquid flow rate, the electrokinetic streaming current is generated within the nozzle aperture by an interaction between the electrical double layer formed at the solid−liquid interface and the fluid velocity profile across the narrow channel. In effect, the flow of liquid strips away the relatively loosely held outer charges of the electrical double layer, leaving an excess of opposite charge more tightly bound to the solid surface of the aperture walls. The excess of charge, both at the aperture walls and carried away by the liquid beam, gives rise to the observed streaming currents having opposite signs.

Measurements of the variation of streaming currents with flow velocity are well established, with reports describing measurements at either the equivalent of our downstream plate[51,59−63] or the nozzle aperture.[35,63,64] There is no report in the literature of simultaneous measurements being made at the plate and the aperture. Most of the previous work in the field has investigated electrokinetic phenomena in low-conductivity combustible fluids flowing through relatively large diameter pipes.[51,59−61] Some theoretical investigation into the electrostatics involved in fluid flow through smaller, millimeter-sized tubes has been reported,[65−67] but there is no report for the expected flow velocity dependence of streaming currents generated in micron-sized apertures.

Figure 2 shows that the dependence of the streaming currents on methanol flow velocity is not linear. Indeed, the nonlinear velocity dependence is identical for current measurements at both the aperture and the plate. The line of best fit in Figure 2 is a quadratic fit to the data. Models have been developed that describe the flow velocity dependence of electrostatic streaming currents in relatively large diameter pipes. Under conditions of laminar flow, Gibbings[59] predicts a linear relationship between flow velocity and streaming current. The clear nonlinear behavior exhibited in Figure 2 is direct evidence that laminar

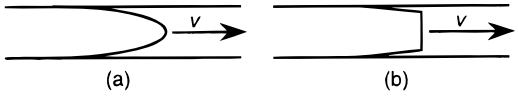

Figure 3. (a) Schematic illustration of the Poiseuille velocity distribution expected under laminar flow conditions. (b) Schematic illustration of the near "top hat" velocity distribution expected under turbulent flow conditions.

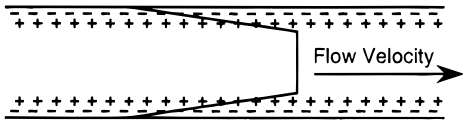

Figure 4. Exaggerated schematic illustration of the spatial overlap between the electric double layer and the turbulent flow velocity gradient at the channel wall. The velocity gradient interacts with the weakly held outer portion of the electric double layer. This initiates the charge separation process manifested as an electrokinetic streaming current.

flow has not been achieved. Several phenomenological models have been proposed to describe the flow velocity dependence under turbulent flow conditions. In 1962 Schoen[68] proposed that the streaming current varies with flow velocity to a power between 1.8 and 2.0. Gibson and Lloyd proposed that[60,61] that the streaming current varies with flow velocity to a power of 2.4. Finally, Klinkenberg[51] proposed that the streaming current varies with flow velocity to a power of 1.9. While each of these phenomenonological models provides little, if any, insight into the microscopic electrohydrodynamic processes at play during the electrokinetic charge separation process, each shows a near-quadratic dependence on flow velocity, as observed in this study. We therefore conclude that the same fundamental physical processes are at play in the turbulent flow of liquids through both large diameter (centimeter- and millimeter-sized) pipes and micron-sized thin apertures. As we shall discuss below, the same cannot be said for laminar flow conditions.

The magnitude of an electrokinetic streaming current depends on the rate at which charge from the outer region of the electric double layer is sheared away from the inner region of charge at the solid−liquid interface. The nonlinear dependence of streaming current with bulk flow velocity is not unexpected. At the boundary between the aperture and the liquid, the fluid flow velocity is zero. Under laminar flow conditions, a parabolic (or Poiseuille) velocity distribution is created across the diameter of the flow channel (see Figure 3a).[57] The center velocity in the Poiseuille distribution is the bulk linear flow velocity. However, under turbulent conditions as experienced in the experiments reported here, plug flow through the channel results. A near "top hat" velocity profile with a flow-front having the bulk flow velocity is generated (see Figure 3b). The velocity gradient at the channel wall is of great significance as it is in this region that the electric double layer exists. An exaggeration of the spatial overlap between the electric double layer and the turbulent flow velocity gradient is schematically illustrated in Figure 4.

The velocity gradient at the channel wall for turbulent flow has been defined as[69]

$$\frac{dv}{dy} = \frac{A\rho v^2}{8\eta R_e^{0.25}} \qquad (5)$$

where v is the bulk flow velocity, ρ is the liquid density, η is the liquid viscosity, R_e is the Reynolds number, A is an empirical constant (equal to 0.3164 under turbulent flow conditions) and y refers to the distance away from the wall. In Figure 5 we present the variation in electrokinetic streaming current with wall velocity gradient. The variation in Figure 5 shows a linear relationship, consistent with the notion that charge separation occurs in this region of rapidly varying flow velocity.

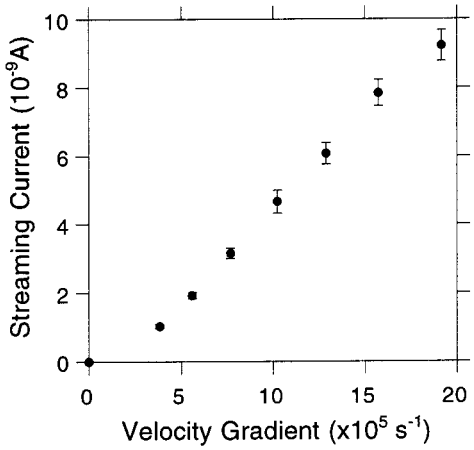

Figure 5. Variation of the electrokinetic streaming current with fluid flow velocity gradient at the channel wall. The data exhibits a near linear dependence. See text for details. Error bars represent one standard deviation.

3.2. Laminar Flow. For electrokinetic streaming current measurements under laminar flow conditions, the 0.5 mm thick stainless steel aperture was replaced by a 3 cm length of fused silica capillary. The internal diameter of the capillary was 25 μm. All other aspects of the apparatus configuration were retained. The only change to the experimental protocol involved limiting measurements of streaming currents to the downstream copper plate. The nonconducting nature of the fused silica capillary not only prevented any measurement of streaming currents at the capillary itself, but as will be discussed later in this section, also influenced the extent of charge separation. In experiments using the electrically conducting stainless steel aperture, excess charge was dissipated through the attached picoammeter. When using the fused silica capillary, excess charge generated by the charge separation process was dissipated to the grounded apparatus through the methanol itself.

In Figure 6 we present the variation of electrokinetic streaming current with bulk flow velocity for twice-distilled methanol. Error bars represent one standard deviation. Measurements were made under laminar flow conditions. The lowest fluid flow rate used for these measurements was 0.2 mL/min, corresponding to a bulk flow velocity of 6.8 m/s. At flow rates less than 0.2 mL/min the liquid microjet ceased to operate. Just as under turbulent flow conditions, the solvent formed small drops around the nozzle exit which rapidly froze the capillary channel closed. The highest fluid flow rate used was 1.2 mL/min, corresponding to a bulk fluid flow velocity of 40.7 m/s. At flow rates greater than 1.2 mL/min, the backing pressure within the solvent delivery pump became excessive.

As for currents measured under turbulent flow conditions, the flow velocity dependence of electrokinetic streaming currents recorded under laminar flow conditions exhibits an apparent strong nonlinearity. The solid line in Figure 6 is a quadratic fit to the data and serves to guide the eye only. Our observation of nonlinearity would appear to be at odds with the predictions of several phenomenological models developed to account for electrokinetic currents generated under laminar flow conditions in large diameter pipes. As mentioned earlier, Gibbings[59] predicted a linear relationship between flow velocity and streaming current. This linear relationship was also predicted

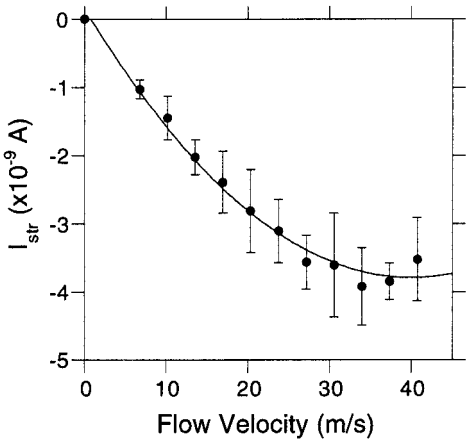

Figure 6. Variation of the electrokinetic streaming current with fluid flow velocity. Data are collected under laminar flow conditions generated by passing twice-distilled methanol through a 3 cm long, 25 μm diameter fused silica capillary. The streaming current generated by excess charge carried away by the liquid beam is measured by connection of a picoammeter to an electrically isolated copper plate located 20 cm downstream from the nozzle orifice. Error bars represent one standard deviation.

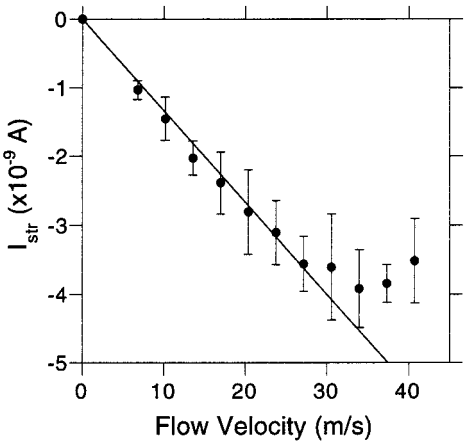

Figure 7. Comparison of the variation of the electrokinetic streaming current with fluid flow velocity under laminar flow conditions with that predicted by the model of Walmsley and Woodford.[70] Models by Gibbings,[59] Walmsley,[71] and Davies[52] give similar results. Clearly there is good agreement at flow velocities less than approximately 30 m/s. Significant deviations from linearity occur at higher velocities where saturation of the charge separation process is evident. See text for details.

by Walmsley and Woodford (who in fact present four distinct model scenarios all predicting a linear response)[70] and later reinforced by Walmsley.[71] Davies[52] has presented a theoretical treatment showing a linear relationship between flow velocity and streaming current under laminar flow conditions.

The phenomenological models cited above all discuss flow conditions through large diameter pipes. The large pipe diameters result in flow velocities that are slower than those considered in this study. In Figure 7 we present a comparison between the observed and one of the predicted electrokinetic streaming currents as a function of flow velocity under laminar conditions. The predicted linear dependence is based upon the "case c" scenario reported by Walmsley and Woodford (the third of the four models presented by these workers).[70] Within experimental error, this comparison shows that a linear relationship between streaming current and flow velocity is observed for velocities less than ~30 m/s. At velocities above about 30 m/s the electrokinetic charge separation process reaches saturation as there is no further dependence of streaming current on bulk flow velocity.

One possible explanation for the observed nonlinear behavior evident in Figures 6 and 7 involves considering the chemical equilibrium established between methanol and the fused silica at the solid−liquid interface. Fused silica is a heterogeneous substance, existing in several crystalline forms as well as being found in an amorphous state.[72] The bulk of the crystalline state consists of three-dimensional chains of alternating silicon and oxygen atoms. At the silica surface these chains usually terminate in hydroxyl groups. The geometrical arrangements of the hydroxyl groups exhibit a variety of configurations, with isolated, vicinal (**1**) and geminal (**2**) silanol groups (the latter two descriptors refer to one or two hydroxyl groups per silicon atom, respectively), and a siloxane, or oxygen bridging, configuration.

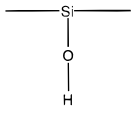

(**1**)

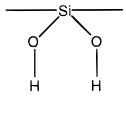

(**2**)

Protons are present in solution as a result of the self-dissociation of methanol itself, as well as any residual water in the system. The extent of electrokinetic charge separation is influenced by the surface charge on the silica. The surface charge is determined by the equilibrium established between protons in solution and surface hydroxyl groups.[73]

$$SiOH_2^+ \rightleftharpoons SiOH + H^+ \quad (6)$$

$$SiOH \rightleftharpoons SiO^- + H^+ \quad (7)$$

The siloxane moieties play no part in binding protons to the silica surface and will not be considered further here.

Proton NMR studies have estimated that 32% of the surface silanol groups are geminal, with the remaining 68% adopting the vicinal structure.[72] The density of hydroxyl groups on the surface has been estimated to vary from 4.6 to 8 per square nanometer, depending on the local structural arrangement.[72] Some uncertainty exists as to the acidity of surface silanol groups in a hydrated environment, with estimates of pK values varying from as low as −0.4 to an average of 7.1.[72] It is believed that the wide variation in apparent silanol acidity arises due to differing acidity constants of the geminal and vicinal species. The heterogeneous nature of silica samples makes it extremely difficult to isolate these species. Nonetheless, because the silanol groups exist in equilibrium with protons in solution, in our model discussed below we assume that a good proportion of the silanol groups are protonated, with terminal $SiOH_2^+$ moieties playing a leading role in the surface electrochemistry.

In our simple model, H^+ ions in solution interact with the fused silica capillary walls where they protonate surface SiOH groups. With the cations removed from the solvent flow, there is an excess of methoxide anions in the liquid beam which gives rise to the electrokinetic streaming currents. Of course, an imbalance of positive electrical charge cannot build up within the capillary indefinitely. In the case of using a stainless steel aperture, excess charge at the aperture was carried away to ground via an attached ammeter. However, in the case of the fused silica capillary, excess electrical charge must be neutralized by back-conduction through the solvent itself to the electrically grounded stainless steel solvent delivery tubing upstream of the capillary. Under low flow velocity conditions,

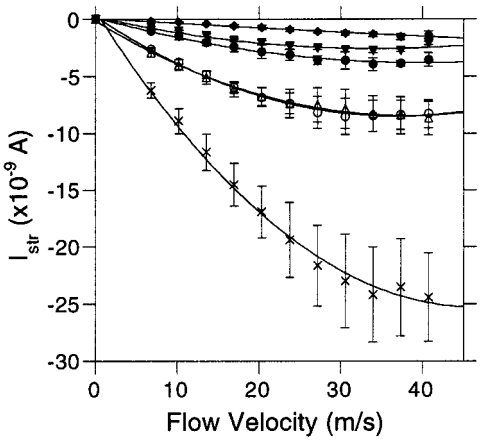

Figure 8. Variation of electrokinetic streaming current with proton concentration. Data are collected under laminar flow conditions generated by passing twice-distilled methanol, to which concentrated HCl is added, through a 3 cm long, 25 μm diameter fused silica capillary. Legend for H^+ concentrations: (◆) 2×10^{-8} M, (▼) 5×10^{-8} M, (●) twice-distilled methanol, (○) 1×10^{-7} M, (△) 1×10^{-6} M, (×) 1×10^{-5} M. The streaming current generated by excess charge carried away by the liquid beam is measured by connection of a picoammeter to an electrically isolated copper plate located 20 cm downstream from the nozzle orifice. Error bars represent one standard deviation.

the buildup of charge within the capillary can be dissipated by back-conduction through the methanol quite readily. As the flow velocity increases, the extent of electrokinetic charge separation increases proportionally until a conduction limit is reached whereby no more excess charge within the capillary can be neutralized. At this point no further charge separation can occur and the saturation in streaming current observed in Figure 7 results. The data in Figure 7 indicates that the conductivity limit for charge neutralization is reached at a mean flow velocity of ~30 m/s.

Having developed the hypothesis that fused silica surface protonation plays an important role in the electrokinetic charge separation process, we investigated the relationship between electrokinetic streaming current and flow velocity for a series of dilute solutions of HCl in methanol. We proposed that an increase in the H^+ concentration in solution would result in a corresponding increase in the extent of silanol protonation, as described by eq 6. Increased silanol protonation would result in a greater degree of charge separation, which in turn would be observed as a larger electrokinetic streaming current (for any given fluid flow velocity).

HCl is a strong acid with a large dissociation constant of 10^7.[74] We expected therefore that the HCl concentration in methanol would be an accurate measure of the actual H^+ concentration. As discussed in later paragraphs, our data shows that this assumption is valid for H^+ concentrations greater than 1×10^{-7} M, but is not necessarily so at very low acid concentrations.

The results of our study into the H^+ concentration dependence on electrokinetic charge generation under laminar flow conditions are presented in Figure 8. The lines of best fit for each concentration data set serve to guide the eye only and have no physical significance. Careful inspection of Figure 8 shows that for each acid concentration, except for perhaps the lowest concentration at 2×10^{-8} M where a near-linear dependency is apparent at all flow velocities, the trend wherein saturation of the streaming current with fluid flow is observed at higher flow velocities. Indeed, saturation of the charge separation process occurs at a mean flow velocity of approximately 30 m/s, irrespective of H^+ concentration. Further studies are required to identify the salient factors influencing the restriction of the back-conduction charge neutralization process. Nonetheless, we conclude that our model involving an interplay between surface protonation, bulk flow velocity, and through-solvent charge neutralization describes the system electrochemistry over at least the 3 orders of magnitude of H^+ concentration investigated here.

Several further aspects concerning the magnitude of streaming currents as a function of H^+ concentration are evident in Figure 8. There is a general trend of an increasing magnitude of streaming current with proton concentration, consistent with the notion of a greater extent of charge separation occurring with more extensive surface protonation. However, the magnitude of the streaming current does not increase with the notional H^+ concentration in every case. Specifically, pure methanol produces a larger streaming current than would be expected from its notional H^+ concentration of $\sim 3 \times 10^{-9}$ M calculated from the reported dissociation constant of 10^{-17}.[75] We account for this apparent anomaly by noting that the pure methanol samples do not contain any chloride counterions from the addition of HCl. The chloride ions reside in the outer region of the surface electrical double layer and, being less strongly held to the surface, are removed in the electrokinetic charge stripping process. Further investigations are planned to interrogate the role of different anions in solution. In any case, at the very low proton concentrations discussed here, we believe that the magnitude of the electrokinetic streaming currents at saturation are a precise measure of the relative concentration of H^+ in solution.

A surprising observation to be made from Figure 8 is that within experimental error, there is absolutely no difference in the variation of streaming current with flow velocity for H^+ concentrations of 1×10^{-7} and 1×10^{-6} M. This intriguing result is entirely reproducible between experimental data runs conducted over a period of several weeks, with different nozzle capillaries and freshly prepared acidic solutions. We attribute this behavior to the differing acidities of the geminal versus vicinal silanol groups at the silica surface. Indeed, our data suggests that the geminal groups undergo preferential protonation relative to the vicinal silanol sites.

We propose that at lower H^+ concentrations the geminal silanol groups preferentially attract protons from solution, initiating the charge separation process. As the H^+ concentration is increased there is a corresponding increase in the magnitude of charge separation; the geminal silanol groups efficiently remove protons from solution. However, at a H^+ concentration of approximately 1×10^{-7} M, proton association saturates the geminal sites, preventing further charge separation. The more prevalent vicinal silanol sites play no part in the charge separation process at these weaker proton concentrations due to their much weaker ability to accept protons from solution. Our model explains the fact that the magnitude of the electrokinetic streaming current observed at a H^+ concentration of 1×10^{-6} M is the same as at 1×10^{-7} M. The excess protons which are not attracted to the silica surface simply exit with the liquid beam. However, as the proton concentration is increased to 1×10^{-5} M, the magnitude of the streaming current again increases. At this higher H^+ concentration the vicinal silanol sites are now available to associate protons from solution, further enhancing the extent of charge separation.

The measurement of electrokinetic streaming currents offers the possibility of providing valuable new insight into surface chemistry structure and dynamics. However, some caution needs

to be exercised when attempting to interpret our results in terms of traditional surface electrochemistry concepts. The magnitude of an electrokinetic streaming potential has been used to describe the degree of charge separation in a Helmholtz double layer by determination of the surface zeta potential.[76] However, in our case, the extremely wide range of acidities of the surface silanol groups, and hence the varying degree of surface charge separation, makes analysis of data in terms of a single value for the electrical double layer (and hence, zeta potential) somewhat problematic. Further theoretical advances describing electrokinetic charging in micron-sized channels is necessary to further understand these phenomena.

4. Conclusions

We have investigated the physicochemical basis of electrokinetic charge separation in methanol using micron-sized channel diameters under both turbulent and laminar flow conditions. Under turbulent flow conditions through a conducting aperture it was determined that the extent of charge separation is proportional to the wall velocity flow gradient. Laminar flow studies were conducted using a 3 cm length of electrically nonconducting fused silica capillary. Under these conditions it was found that saturation of the charge separation process occurs at mean flow velocities greater than approximately 30 m/s. Saturation of the electrokinetic charging process occurs because dissipation of excess charge built up within the capillary walls by back-conduction through the methanol reaches a limiting capacity. We have developed a simple model which shows that, prior to saturation of the charge separation process, the extent of electrokinetic charge separation is controlled by the extent of protonation of silanol sites at the fused silica walls. Further experiments are planned to more fully investigate the complex liquid−surface interfacial electrochemical processes.

Acknowledgment. This work was supported by the University of Adelaide, the South Australian Department of Mines and Energy through the State Energy Research Advisory Committee (SENRAC), and the Land and Water Resources Research and Development Corp. (LWRRDC). We thank Mr. M. Tattersall for early contributions to this work. We also thank Dr. P. Attard, Dr. B. S. Saunders, and Ms. J. M. Weeks for helpful discussions. The technical support provided by the University of Adelaide Mechanical, Electronics, and Glassblowing Workshops is gratefully acknowledged.

References and Notes

(1) Lienau, C.; Zewail, A. H. *J. Phys. Chem.* **1996**, *100*, 18629−18649.
(2) Cheng, P. Y.; Zhong, D.; Zewail, A. H. *J. Chem. Phys.* **1996**, *105*, 6216- 6248.
(3) Fleming, G. R.; Cho, M. H. *Annu. Rev. Phys. Chem.* **1996**, *47*, 109−134.
(4) Joo, T. H.; Jia, Y. W.; Yu, J. L.; Lang, M. J.; Fleming, G. R. *J. Chem. Phys.* **1996**, *104*, 6089−6108.
(5) Sitzmann, E. V.; Eisenthal, K. B. *J. Phys. Chem.* **1988**, *92*, 4579−4580.
(6) Goh, M. C.; Hicks, J. M.; Kemnitz, K.; Pinto, G. R.; Bhattacharyya, K.; Eisenthal, K. B.; Heinz, T. F. *J. Phys. Chem.* **1988**, *92*, 5074−5075.
(7) Zhao, X.; Subrahmanyan, S.; Eisenthal, K. B. *Chem. Phys. Lett.* **1990**, *171*, 558−562.
(8) Eisenthal, K. B. *J. Phys. Chem.* **1996**, *100*, 12997−13006.
(9) Eisenthal, K. B. *Chem. Rev.* **1996**, *96*, 1343−1360.
(10) Eisenthal, K. B. *Acc. Chem. Res.* **1993**, *26*, 636−643.
(11) Lundholm, M.; Siegbahn, H.; Holmberg, S.; Arbman, M. *J. Electron Spectrosc. Relat. Phenom.* **1986**, *40*, 163−180.
(12) Moberg, R.; Bökman, F.; Bohman, O.; Siegbahn, H. O. G. *J. Chem. Phys.* **1991**, *94*, 5226−5232.
(13) King, M. E.; Nathanson, G. M.; Hanning-Lee, M. A.; Minton, T. K. *Phys. Rev. Lett.* **1993**, *70*, 1026−1029.
(14) Saecker, M. E.; Nathanson, G. M. *J. Chem. Phys.* **1993**, *99*, 7056−7075.
(15) *Atomic and Molecular Beam Methods*; Scoles, G., Ed.; Oxford University Press: New York, 1988; Vol. 1.
(16) Serxner, D.; Dessent, C. E.; Johnson, M. A. *J. Chem. Phys.* **1996**, *105*, 7231.
(17) Bailey, C. G.; Kim, J.; Johnson, M. A. *J. Phys. Chem.* **1996**, *100*, 16782.
(18) Choi, J. H.; Kuwata, K. T.; Yao, Y. B.; Okumura, M. *J. Phys. Chem. A* **1998**, *102*, 503.
(19) Ayotte, P.; Bailey, C. G.; Kim, J.; Johnson, M. A. *J. Chem. Phys.* **1998**, *108*, 444.
(20) Bieske, E. J.; Soliva, A. M.; Maier, J. P. *J. Chem. Phys.* **1991**, *94*, 4749.
(21) Bieske, E. J.; Soliva, A. M.; Friedmann, A.; Maier, J. P. *J. Chem. Phys.* **1992**, *96*, 28.
(22) Lessen, D. E.; Asher, R. L.; Brucat, P. J. *J. Chem. Phys.* **1990**, *93*, 6102.
(23) Lessen, D. E.; Asher, R. L.; Brucat, P. J. *J. Chem. Phys.* **1991**, *95*, 1414.
(24) Weinheimer, C. J.; Lisy, J. M. *Int. J. Mass Spectrosc. Ion Processes* **1996**, *159*, 197.
(25) Coe, J. V.; Lee, G. H.; Eaton, J. G.; Arnold, S. T.; Sarkas, H. W.; Bowen, K. H.; Ludewigt, C.; Haberland, H.; Worsnop, D. R. *J. Chem. Phys.* **1990**, *92*, 3980.
(26) Siegbahn, H.; Siegbahn, K. *J. Electron Spectrosc. Relat. Phenom.* **1973**, *2*, 319- 325.
(27) Keller, W.; Morgner, H.; Müller, W. A. *Mol. Phys.* **1986**, *57*, 623−636.
(28) Keller, W.; Morgner, H.; Müller, W. A. *Mol. Phys.* **1986**, *58*, 1039−1052.
(29) Morgner, H.; Oberbrodhage, J.; Ritcher, K.; Roth, K. *J. Phys. Condens. Matter* **1991**, *3*, 5639−5655.
(30) Nishi, N.; Yamamota, K.; Shinohara, H.; Nagashima, U.; Okuyama, T. *Chem. Phys. Lett.* **1985**, *122*, 599−604.
(31) Nishi, N.; Yamamoto, K. *J. Am. Chem. Soc.* **1987**, *109*, 7353−7361.
(32) Yamamoto, K.; Nishi, N. *J. Am. Chem. Soc.* **1990**, *112*, 549−558.
(33) Faubel, M.; Schlemmer, S.; Toennies, J. P. *Z. Phys. D* **1988**, *10*, 269−277.
(34) Faubel, M.; Kisters, T. *Nature* **1989**, *339*, 527−529.
(35) Faubel, M.; Steiner, B. *Ber. Bunsen-Ges. Phys. Chem.* **1992**, *96*, 1167.
(36) Faubel, M.; Steiner, B.; Toennies, J. P. *Mol. Phys.* **1996**, *90*, 327−344.
(37) Faubel, M.; Steiner, B.; Toennies, J. P. *J. Chem. Phys.* **1997**, *106*, 9013−9031.
(38) Mafuné, F.; Takeda, Y.; Nagata, T.; Kondow, T. *Chem. Phys. Lett.* **1992**, *199*, 615−620.
(39) Mafuné, F.; Kohno, J.; Nagata, T.; Kondow, T. *Chem. Phys. Lett.* **1994**, *218*, 7−12.
(40) Mafuné, F.; Takeda, Y.; Nagata, T.; Kondow, T. *Chem. Phys. Lett.* **1994**, *218*, 234−239.
(41) Kohno, J.; Mafuné, F.; Kondow, T. *J. Am. Chem. Soc.* **1994**, *116*, 9801- 9802.
(42) Mafunè, F.; Kohno, J.; Kondow, T. *J. Chin. Chem. Soc.* **1995**, *42*, 449−454.
(43) Matsumura, H.; Mafunè, F.; Kondow, T. *J. Phys. Chem.* **1995**, *99*, 5861- 5864.
(44) Kohno, J.; Horimoto, N.; Mafunè, F.; Kondow, T. *J. Phys. Chem.* **1995**, *99*, 15627−15632.
(45) Mafunè, F.; Hashimoto, Y.; Hashimoto, M.; Kondow, T. *J. Phys. Chem.* **1995**, *99*, 13814−13818.
(46) Horimoto, N.; Mafunè, F.; Kondow, T. *J. Phys. Chem.* **1996**, *100*, 10046- 10049.
(47) Mafunè, F.; Kohno, J.; Kondow, T. *J. Phys. Chem.* **1996**, *100*, 10041−10045.
(48) Mafunè, F.; Kohno, J.; Kondow, T. *J. Phys. Chem.* **1996**, *100*, 4476−4479.
(49) Horimoto, N.; Mafunè, F.; Kondow, T. *Chem. Lett.* **1997**, 159−160.
(50) Mafunè, F.; Hashimoto, Y.; Kondow, T. *Chem. Phys. Lett.* **1997**, *274*, 127- 132.
(51) *Electrostatics in the Petroleum Industry*, 1st ed.; Klinkenberg, A., Van Der Minne, J. L., Eds.; Elsevier: Amsterdam, 1958.
(52) Davies, J. T.; Rideal, E. K. *Interfacial Phenomena*, 2nd ed.; Academic Press: New York, 1963.
(53) Gavis, J.; Koszman, I. *J. Colloid Sci.* **1961**, *16*, 375−391.
(54) Giancoli, D. C. *Physics for Scientists and Engineers with Modern Physics*, 2nd ed.; Prentice Hall: London, 1988.
(55) Aylward, G. H.; Findlay, T. J. V. *SI Chemical Data*, 1st ed.; John Wiley & Sons Australasia: Sydney, 1971.

(56) James, A. M.; Lord, M. P. *Macmillan's Chemical and Physical Data*, 1st ed.; Macmillan: London, 1992.
(57) Levich, V. G. *Physicochemical Hydrodynamics*, 1st ed.; Prentice Hall: Englewood Cliffs, NJ, 1962.
(58) Abedian, B.; Sonin, A. A. *J. Fluid Mech.* **1982**, *120*, 199−217.
(59) Gibbings, J. C. "Interaction of electrostatics and fluid motion"; Presented at the 5th Conference on Static Electrification, Oxford, UK, 1979.
(60) Gibson, N. "Static in fluids"; Presented at the 3rd Conference on Static Electrification, London, 1971.
(61) Gibson, N.; Lloyd, F. C. *J. Phys. D.; Appl. Phys.* **1970**, *3*, 563−575.
(62) Klinkenberg, A. *Chem.-Ing.-Techn.* **1964**, *36*, 283−290.
(63) Keller, H. N.; Hoelscher, H. E. *Ind. Eng. Chem.* **1957**, *49*, 1433−1438.
(64) Koszman, I.; Gavis, J. *Chem. Eng. Sci.* **1962**, *17*, 1023−1040.
(65) Malik, S. K.; Singh, M. *Q. Appl. Math.* **1983**, *41*, 273−287.
(66) Kant, R.; Malik, S. K. *Q. Appl. Math.* **1986**, *43*, 407−419.
(67) Mestel, A. J. *J. Fluid Mech.* **1994**, *274*, 93−113.
(68) Schoen, G. *Chem.-Ing.-Techn.* **1962**, *34*, 432.
(69) Hignett, E. T.; Gibbings, J. C. *J. Electroanal. Chem.* **1968**, *16*, 239−249.
(70) Walmsley, H. L.; Woodford, G. *J. Phys. D: Appl. Phys.* **1981**, *14*, 1761−1782.
(71) Walmsley, H. L. "Charge generation in low dielectric constant liquids". Presented at the Electrostatics Conference, Oxford, UK, 1983.
(72) Cox, G. B. *J. Chromatogr. A* **1993**, *656*, 353−367.
(73) Grieser, F.; Lamb, R. N.; Wiese, G. R.; Yates, D. E.; Cooper, R.; Healy, T. W. *Radiat. Phys. Chem.* **1984**, *23*, 43−48.
(74) Albert, A.; Serjeant, E. P. *Ionisation Constants of Acids and Bases*; Methuen: London, 1962.
(75) Dobos, D. *Electrochemical Data: A Handbook for Electrochemists in Industry and Universities*; Elsevier: New York, 1975.
(76) Shaw, D. J. *Introduction to Colloid and Surface Chemistry*, 2nd ed.; Butterworth Heinemann: Oxford, UK, 1992.